Image reconstruction based on approximate function and modified conjugate gradient

Ping Gong*

School of Information and Electronic Engineering,
Wuzhou University,
Wuzhou Guangxi 543002, China
and
Guangxi Colleges and Universities Key Laboratory of Image Processing and Intelligence Information System,
Wuzhou University,
Wuzhou Guangxi 543002, China
Email: pinggong@21cn.com
*Corresponding author

Guohua Li and Jian Li

School of Information and Electronic Engineering,
Wuzhou University,
Wuzhou Guangxi 543002, China
Email: weiqqi9@sina.com
Email: jianli007@21cn.com

Abstract: This paper proposed an approach combines the advantages of L1 norm and TV norm by combining L1 norm and TV norm to solve the image reconstruction problems. And the proposed approach reconstructs an image from the measured values by using the modified conjugate gradient algorithm for the purpose of improving the efficiency of image reconstruction. The objective function is constructed using the approximate function based on the L1 norm and TV norm. A sparse transformation is applied to the original image first. The random Gaussian matrix is then employed to perform a compressive measurement on the 2-D sparse signal. To reconstruct the image a regularised reconstruction model is established through the approximate norm that combines L1 norm and TV norm and the gradient of the approximate norm is computed. The simulation results demonstrate the ability of the proposed method to reconstruct images more effectively and produce better results in terms of objective indicators such as PSNR and SSIM than classical methods.

Keywords: compressive sensing; L1 norm; total variation; modified conjugate gradient algorithm; image reconstruction.

Reference to this paper should be made as follows: Gong, P., Li, G. and Li, J. (2020) 'Image reconstruction based on approximate function and modified conjugate gradient', *Int. J. Computing Science and Mathematics*, Vol. 11, No. 1, pp.93–105.

Biographical notes: Ping Gong works in the School of Information and Electronic Engineering of Wuzhou Universtity, Wuzhou Guangxi China and also works in Guangxi Colleges and Universities Key Laboratory of Image Processing and Intelligence Information System of Wuzhou Universtity. She is now an Associate Professor, whose research interest is image processing.

Guohua Li works in the School of Information and Electronic Engineering of Wuzhou Universtity, Wuzhou Guangxi China. His research interest is image processing.

Jian Li works in the School of Information and Electronic Engineering of Wuzhou Universtity, Wuzhou Guangxi China. He is a Lecturer, whose research interest is image processing.

1 Introduction

The compressed sensing (CS) theory (Donoho, 2006a; Candes et al., 2006) overcomes the limits of the traditional sampling theorem. If the sampled signal is sparse itself or sparse over a transform domain, then a non-coherence observation matrix can be used to directly collect a small amount of observed data. The original signal can then be reconstructed at a high probability from the small amount of observed data by solving an optimisation problem, according to the CS theory. The CS theory mainly involves three key technologies: sparse representation of signals, construction of the observation matrix and the reconstruction algorithm. The research in CS is mainly focused on the reconstruction algorithm. Reconstructing the spare signal using CS measured values can be considered as the problem of finding the sparsest solution to the underdetermined system of equations. This involves an optimisation of the L0 norm, which is considered an NP-hard problem (Donoho and Tsaic, 2006). In recent years, research has focused on CS-based reconstruction of sparse signals and many reconstruction algorithms were proposed. Some of these algorithms rely on solving the convex optimisation problem. The gradient projection algorithm (Figueiredo et al., 2007) and the linearised Bregman iterative methods (Chen et al., 2016b) are examples of such algorithms.

The most widely used in all kinds of convex optimisation algorithms is the least square problem based on L1 norm. It is theoretically proven that under certain conditions, the non-convex L0 norm-based least square problem can be converted into a convex L1 norm-based least square problem (Donoho and Tsaic, 2006; Donoho, 2006b). The Nesterov smoothing technique was used in Chen and Li (2016) to build the approximate function of the L1 norm and the modified HS conjugate gradient method is used to solve the least square problem, moreover, an inexact linear search strategy was adopted for large-scale signal restoration. Figueiredo et al. (2007) proposed to address the L1 norm-based least square problem using the gradient projection method. Their algorithm proofed to reconstruct signals more effectively and more quickly than some methods.

In addition to preserving edge characteristics, the TV regularisation strategy is further able to eliminate noise very effectively (Chen et al., 2016a). In recent years, the TV norm-based least square algorithm has also been applied to the reconstruction of CS signals. A non-local regularisation method was proposed in Zhang et al. (2012) to improve the image reconstruction performance of the TV norm-based CS signals. Jeevan

et al. (2013s) proposed a new method called TVp_RLS to address the least square problem. The method is based on the minimisation of the TV regularised squared error and represents the TVP norm using the approximate function. The image is in this case reconstructed using the FR conjugate gradient method and the linear search method based on the Banach fixed point theorem jointly. This method is well suited for image reconstruction from a small number of measurements.

In this paper, after jointly considering the signal's sparsity and the target image's gradient variation, a least square method that combines L1 regularisation and TV regularisation is proposed to represent the objective function for compressive reconstruction of images. Moreover, the norm computation is replaced with an approximate function. A modified conjugate gradient method is then used to reconstruct the image. The results showed better visual effects than classical methods in an objective assessment.

In the follow of this paper, the typical data acquisition model in CS and the classical reconstruction models are introduced in Section 2. In the Section 3, the proposed approach combined the L1 norm and TV norm is presented. In the proposed method, an image is reconstructed using the modified conjugate gradient algorithm. In the Section 4, the experiments and simulation results are displayed.

2 Compressed sensing

In this section, we introduce the typical data acquisition model in CS and the classical reconstruction models.

As mentioned in Section 1, CS is a signal processing technique for efficiently acquiring and reconstructing a signal, by finding solutions to underdetermined linear systems.

Consider an $n \times m$ 2D sparse signal X and an $M \times n$ observation matrix Φ that meets the restricted isometry property (RIP). Measuring X yields $M \times m$ 2D measured values Y. In CS, a typical data acquisition model is given by:

$$Y = \Phi X \tag{1}$$

where $M < n$.

While reconstructing X via Y, we need to address a constrained L_0 norm optimisation problem, which is described as follows

$$\min \|X\|_0 \quad \text{s.t.} \Phi X = Y \tag{2}$$

The non-convex optimisation problem in equation (2) can be converted into a convex optimisation problem by solving the following L1 norm optimisation problem:

$$\min \|X\|_1 \quad \text{s.t.} \Phi X = Y \tag{3}$$

Assuming the matrix Φ is full row rank, the constrained minimisation problem in Equation (3) can be converted into the following L1 regularised least square problem:

$$\min \left\{ \alpha \|X\|_1 + \frac{1}{2} \|\Phi X - Y\|_2^2 \right\} \tag{4}$$

where α denotes the regularisation parameter.

The problem in equation (1) can also be addressed using the TV regularisation method:

$$\min\left\{\alpha\|X\|_{TV}+\frac{1}{2}\|\Phi X-Y\|_2^2\right\} \tag{5}$$

The TV norm can be either isotropic or anisotropic. The isotropic TV norm of X can be defined as (Beck and Teboulle, 2009):

$$\begin{aligned}\|X\|_{ITV} &= \sum_{i=1}^{n-1}\sum_{j=1}^{m-1}\sqrt{\left(X_{i,j}-X_{i+1,j}\right)^2+\left(X_{i,j}-X_{i,j+1}\right)^2}\\ &+\sum_{i=1}^{n-1}\left|X_{i,m}-X_{i+1,m}\right|+\sum_{j=1}^{m-1}\left|X_{n,j}-X_{n,j+1}\right|\end{aligned} \tag{6}$$

The anisotropic of TV norm is defined as (Ibrahim et al., 2015):

$$\begin{aligned}\|X\|_{ATV} &= \sum_{i=1}^{n-1}\sum_{j=1}^{m-1}\left(\left|X_{i,j}-X_{i+1,j}\right|+\left|X_{i,j}-X_{i,j+1}\right|\right)\\ &+\sum_{i=1}^{n-1}\left|X_{i,m}-X_{i+1,m}\right|+\sum_{j=1}^{m-1}\left|X_{n,j}-X_{n,j+1}\right|\end{aligned} \tag{7}$$

3 The proposed algorithm

In CS, L1 norm or TV norm is usually but individually used to solve the signal reconstruction problems. Considered combining the norms to solve signal reconstruction problems together so that the algorithm can get more advantages.

The proposed approach constructs objective function using the approximate function of the L1 norm and TV norm. L1 norm is used to control the reconstructed signal's sparsity and the TV norm is used to constrain the reconstructed signal's gradient variation and to preserve edge characteristics. Also, the proposed approach reconstructs an image from the measured values using the modified conjugate gradient algorithm.

3.1 Objective function combining L1 norm and TV norm

To reconstruct the CS images, a new regularisation method that combines the L1 norm and the TV norm is proposed. As shown in equation (8), the L1 norm is used to control the reconstructed signal's sparsity and the TV norm is used to constrain the reconstructed signal's gradient variation:

$$\min\left\{u\|X\|_1+\delta\|X\|_{TV}+\frac{1}{2}\|\Phi X-Y\|_2^2\right\} \tag{8}$$

where μ and δ denote the regularisation parameters. Considering $\mathrm{TV}(X) = \delta\|X\|_{TV}$, $\mathrm{L1}(X) = u\|X\|_1$, $\mathrm{G}(X) = u\|X\|_1+\delta\|X\|_{TV}$, $\mathrm{J}(X) = u\|X\|_1+\delta\|X\|_{TV}+\frac{1}{2}\|\Phi * X-Y\|_2^2$, equation (8) can be written as:

$$\min\left\{G(X)+\frac{1}{2}\|\Phi X-Y\|_2^2\right\} \tag{9}$$

3.2 Approximate function and gradient

The approximate function is used to substitute L1(X) and TV(X), G(X) is written as:

$$G_{\tau,c}(X)=\mu\sum_{i=1}^{n}\sum_{i=1}^{m}\left(X_{i,j}^{2}+\tau^{2}\right)^{1/2}+\delta\sum_{i=1}^{n}\sum_{i=1}^{m}\left(\nabla^{2}+c^{2}\right)^{1/2} \tag{10}$$

where the parameters $\tau > 0$ and $c > 0$ hold, thus, $G_{\tau,c}(X)$ is differentiable. ∇ denotes the gradient of X_{ij}. And then, the gradient of $G_{\tau,c}(X)$ is given by:

$$\nabla G_{\tau,c}\left(X_{i,j}\right)=\frac{\partial G_{\tau,c}\left(X_{i,j}\right)}{\partial X_{i,j}}=\mu\frac{X_{ij}}{\sqrt{X_{i,j}{}^{2}+c^{2}}}+\delta\frac{\nabla}{\sqrt{\nabla^{2}+c^{2}}} \tag{11}$$

The horizontal gradient H and vertical gradient V of the image X need to be computed before obtaining the gradient of $G_{\tau,c}(X)$.

$$H_{i,j}=X_{i,j}-X_{i,j+1} \tag{12}$$

$$V_{i,j}=X_{i,j}-X_{i+1,j} \tag{13}$$

Notice that, different $X_{i,j}$ has different ∇. So, $\frac{\nabla}{\sqrt{\nabla^{2}+c^{2}}}$ would be consisted by different items. For example, considering the $X_{i,j}$ in the top left corner of the image, the $\frac{\nabla}{\sqrt{\nabla^{2}+c^{2}}}$ was consisted by two items:

$$\begin{aligned}\frac{\nabla}{\sqrt{\nabla^{2}+c^{2}}}&=\frac{X_{i,j}-X_{i,j+1}}{\sqrt{\left(X_{i,j}-X_{i,j+1}\right)^{2}+c^{2}}}+\frac{X_{i,j}-X_{i+1,j}}{\sqrt{\left(X_{i,j}-X_{i+1,j}\right)^{2}+c^{2}}}\\&=H_{i,j}\left(H_{i,j}^{2}+c^{2}\right)^{-1/2}+V_{i,j}\left(V_{i,j}^{2}+c^{2}\right)^{-1/2}\end{aligned} \tag{14}$$

And if the $X_{i,j}$ is in the top boundary of the image, then

$$\begin{aligned}\frac{\nabla}{\sqrt{\nabla^{2}+c^{2}}}&=\frac{X_{i,j}-X_{i,j+1}}{\sqrt{\left(X_{i,j}-X_{i,j+1}\right)^{2}+c^{2}}}+\frac{X_{i,j}-X_{i+1,j}}{\sqrt{\left(X_{i,j}-X_{i+1,j}\right)^{2}+c^{2}}}\\&\quad-\frac{X_{i,j-1}-X_{i,j}}{\sqrt{\left(X_{i,j-1}-X_{i,j}\right)^{2}+c^{2}}}\\&=H_{i,j}\left(H_{i,j}^{2}+c^{2}\right)^{-1/2}+V_{i,j}\left(V_{i,j}^{2}+c^{2}\right)^{-1/2}-H_{i,j-1}\left(H_{i,j-1}^{2}+c^{2}\right)^{-1/2}\end{aligned} \tag{15}$$

So, the gradient $\nabla G_{\tau,c}(X_{i,j})$ of $G_{\tau,c}(X)$ can be computed in the following ways.

$$Q_{1}=H_{i,j}\left(H_{i,j}^{2}+c^{2}\right)^{-1/2} \tag{16a}$$

$$Q_{2}=V_{i,j}\left(V_{i,j}^{2}+c^{2}\right)^{-1/2} \tag{16b}$$

$$Q_{3}=H_{i,j-1}\left(H_{i,j-1}^{2}+c^{2}\right)^{-1/2} \tag{16c}$$

$$Q_4 = V_{i,j-1}\left(V_{i-1,j}^2 + c^2\right)^{-1/2} \tag{16d}$$

$$Q_5 = \left(X_{i,j}^2 + \tau^2\right)^{-1/2} X_{i,j} \tag{16e}$$

$$\nabla G_{\tau,c}\left(X_{i,j}\right) = \begin{cases} \delta\left(Q_1 + Q_2\right) + \mu Q_5 & i = 1,\ j = 1 \\ \delta\left(Q_1 + Q_2 - Q_3\right) + \mu Q_5 & i = 1,\ 2 \le j \le m-1 \\ \delta\left(Q_1 + Q_2 - Q_4\right) + \mu Q & 2 \le i \le n-1,\ j = 1 \\ \delta\left(Q_1 + Q_2 - Q_3 - Q_4\right) + \mu Q_5 & 2 \le i \le n-1 \\ & 2 \le j \le m-1 \\ \delta\left(Q_1 - Q_3 - Q_4\right) + \mu Q_5 & i = n,\ 2 \le j \le m-1 \\ \delta\left(Q_2 - Q_3 - Q_4\right) + \mu Q_5 & 2 \le i \le n-1,\ j = m \\ \delta\left(-Q_3 - Q_4\right) + \mu Q_5 & i = n,\ j = m \\ \delta\left(Q_1 - Q_3\right) + \mu Q_5 & i = n,\ j = 1 \\ \delta\left(Q_2 - Q_4\right) + \mu Q_5 & i = 1,\ j = m \end{cases} \tag{17}$$

The gradient $\nabla J(X)$ of $J(X)$ is:

$$\begin{aligned} \nabla J(X) &= \nabla G_{\tau,c}(X) + \Phi^T(\Phi X - Y) \\ \nabla J(X) &= \Phi^T \Phi X - \Phi^T Y + \nabla G_{\tau,c}(X) \end{aligned} \tag{18}$$

In order to obtain $\min\{J(X)\}$, let $\nabla J(X)$ and we have:

$$\begin{aligned} \nabla G_{\tau,c}(X) + \Phi^T(\Phi X - Y) &= 0 \\ \Phi^T \Phi X &= \Phi^T Y - \nabla G_{\tau,c}(X) \end{aligned} \tag{19}$$

Considering $A = \Phi^T\Phi$, $b = \Phi^T Y - \nabla G_{\tau,c}(X)$, equation (19) can be written as:

$$AX = b \tag{20}$$

3.3 Image reconstruction based on the modified conjugate gradient method

The conjugate gradient method is an important optimisation method. The classical conjugate gradient methods include FR, PRP, HS, DY, CD and so on (Ibrahim et al., 2015). These algorithms vary in terms of the search direction d_k, the search strategy, the calculation of the step length λ_k and the parameter β_k.

A modified conjugate gradient method is used in this paper to solve the minimisation problem given in equation (8). The approximate value of X is determined by iteratively computing equation (21) until $\left\|g_{k+1}\right\|^2 \le \varepsilon$ 1e-7 or the pre-defined maximum number of iterations *Max* is reached.

$$X_{k+1} = X_k + \lambda_k d_k \tag{21}$$

where d_k denotes the search direction, $\lambda_k \geq 0$ denotes the search step length and g_k denotes the gradient of $J(X)$ which can be computed through equation (18).

Vol. 11, No. 1,A strategy was proposed in Cheng and Liu (2010) to determine the search direction:

$$d_k = \begin{cases} -g_k & k = 1 \\ -\left(1 + \beta_k \dfrac{g_k^T d_{k-1}}{\|g_k\|^2}\right) g_k + \beta_k d_{k-1} & k \geq 2 \end{cases} \tag{22}$$

The search direction determined in this way satisfies the sufficient descent property and is independent of linear search and the choice of β_k. Based on this, equation (23) is proposed to compute β_k. Regarding the 2D signal X (a matrix), the value of λ_k is determined using the simple and feasible strategy of exact search.

$$\beta_k = \frac{g_k^T (g_k - g_{k-1})}{g_k^T g_{k-1}} \tag{23}$$

$$\lambda_k = -\frac{g_k^T d_k}{d_k^T A d_k} \tag{24}$$

4 Experimental results and analysis

Simulations have been performed on typical test images like Lena, Barbara and Baboon. All the algorithms were run on a PC desktop with Intel Core i7-6700 3.40GHz CPU and 8.00GB memory and MATLAB R2013a. A sparse representation is obtained from the original image through discrete cosine transform (DCT) and compressed sampling is done via the Gaussian random matrix. The sampling rates are 0.3, 0.4, 0.5, 0.6, 0.7, 0.8 and 0.9. The following parameters were set: μ = 0.0001, δ = 0.0001, c = 1e-4, τ = 1e-4, ε = 1e-7 and the maximum number of iterations were fixed at Max = 10,000. Evaluation indicators of the reconstructed images include the peak signal-to-noise ratio (PSNR) and the structural similarity (SSIM).

Some of the reconstructed images are shown in Figure 1 and the indicators PSNR and SSIM of the reconstructed images are given in Table 1.

Figure 1 and Table 1 show that the quality of the reconstructed images increases with the sampling rate. The reconstructed image Lena is very clear and the edges are well preserved at a sampling rate of 0.6 under a certain Gaussian random matrix. For a sampling rate of 0.3, the accuracy is $\|g_k\|^2 \leq \varepsilon$ 1e-7 after 7,729 iterations which yield a PSNR of 22.9280 dB and a SSIM of 0.9333. The reconstructed image shows degradation when compared with the original image but it is still identifiable.

Figure 1 Images reconstructed using the proposed method, (a) original Lena (b) sampling rate of 0.9 (c) sampling rate of 0.8 (d) sampling rate of 0.7 (e) sampling rate of 0.6 (f) sampling rate of 0.5 (g)sampling rate of 0.4 (h) sampling rate of 0.3

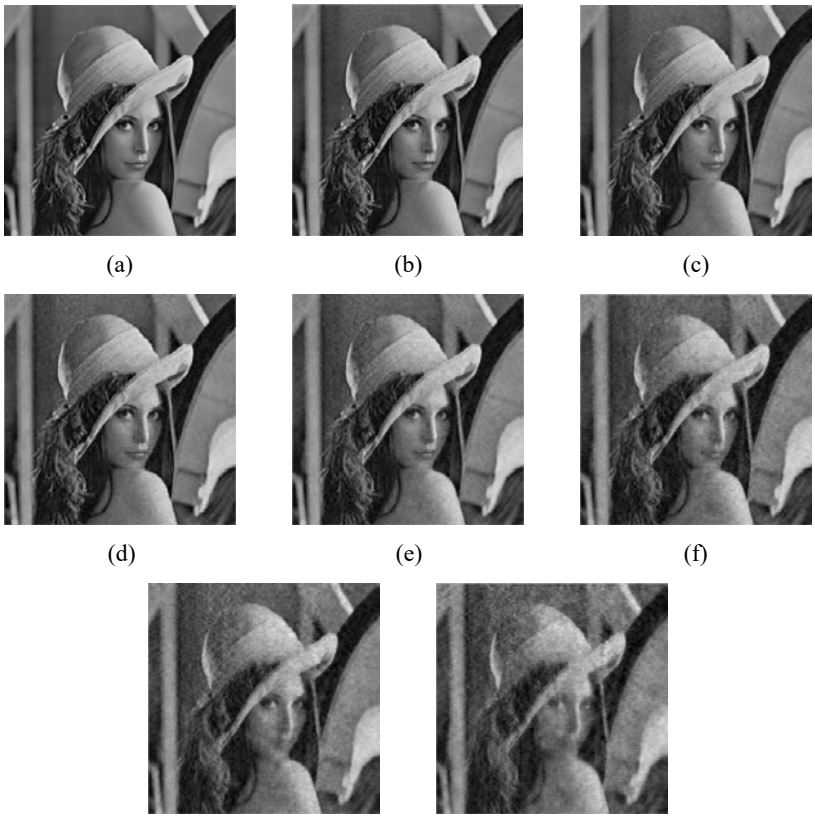

Table 1 Objective evaluation of the reconstructed image Lena

Sampling rate	*PSNR*	*SSIM*	*Number of iterations*
0.9	37.1973	0.9977	2,816
0.8	33.6570	0.9949	3,594
0.7	31.2443	0.9910	4,651
0.6	28.9044	0.9844	1,541
0.5	26.9786	0.9753	3,120
0.4	24.8927	0.9591	6,089
0.3	22.9280	0.9333	7,729

To further evaluate the reconstruction performance of the proposed method, experiments were conducted on the following images: Lena (256 × 256 pixel), Baboon (256 × 256 pixel), Barbara (512 × 512 pixel), Pepper (512 × 512 pixel) and Boats (1,024 × 1,024 pixel). Regarding the regularisation and the conjugate gradient, the proposed method is compared with the algorithm L1_PRP that combines L1 norm and PRP conjugate

gradient method and the algorithm TV_PRP that combines TV norm and PRP conjugate gradient method. The high-resolution image which is larger than 256 × 256 is equally divided into several 256 × 256 sub-images and each of them is then subjected to discrete cosine transform. A fixed Gaussian random matrix is applied for compressed sampling. The sampling rate is set to 0.6, the other parameters are set as follows Max = 5,000, c = 1e-4, τ = 1e-4, μ = 0.0001, δ = 0.0001 and ε = 1e-7. Some examples of the experimental results are given in Figures 2, 3 and 4. PSNR and SSIM indicators are shown in Table 2.

Figure 2 Image Lena reconstructed at a sampling rate of 0.6, (a) original image of Lena (b) proposed method (c) L1_PRP (d) TV_PRP

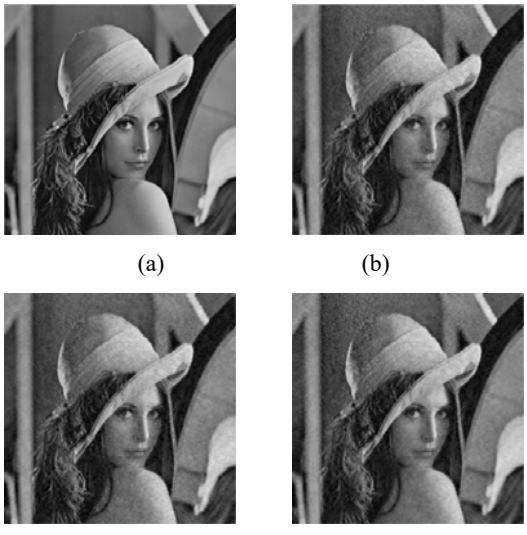

(a) (b)

(c) (d)

Table 2 PSNR and SSIM indicators of the image reconstructed at a sampling rate of 0.6

Image	*Proposed*	*L1_PRP*	*TV_PRP*
Lena	28.9551/0.9846	28.5382/0.9831	28.1480/0.9815
Baboon	20.8270/0.8816	19.9401/0.8566	20.5156/0.8749
Barbara	29.9350/0.9888	28.8866/0.9857	29.2354/0.9868
Pepper	31.6494/0.9923	31.0857/0.9912	30.7510/0.9905
Boats	37.8457/0.9975	36.6591/0.9968	36.8523/0.9969

The results in Figures 2, 3 and 4, show that images reconstructed using the proposed method are similar to those reconstructed using L1_PRP and TV_PRP. But considering the PSNR and SSIM indicators, the proposed method exceeds the results given by L1_PRP and TV_PRP. Hence, the proposed method is able to provide better reconstruction performance for various resolution ratios.

Consider the image Lena at a sampling rate of 0.6. Figure 5 shows the relation between the reconstruction effectiveness and the number of iterations for the three methods, (i.e., the proposed method, L1_PRP and TV_PRP).

Figure 3 Image baboon reconstructed at a sampling rate of 0.6, original image of baboon (b) proposed method (c) L1_PRP (d) TV_PRP

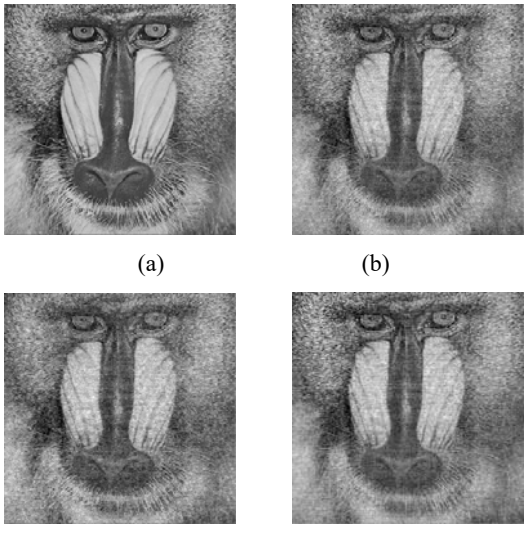

(a) (b)

(c) (d)

Figure 4 Reconstructed image Barbara at a sampling rate of 0.6, original image of Barbara (b) proposed method (c) L1_PRP (d) TV_PRP

(a) (b)

(c) (d)

Figure 5 shows that the reconstruction performance increases with the iterations. After 2,100 iterations, the proposed method in terms of PSNR and SSIM exceeds L1_PRP and TV_PRP.

Figure 5 Objective assessment of the images reconstructed at a sampling rate of 0.6, (a) PSNR (b) SSIM (see online version for colours)

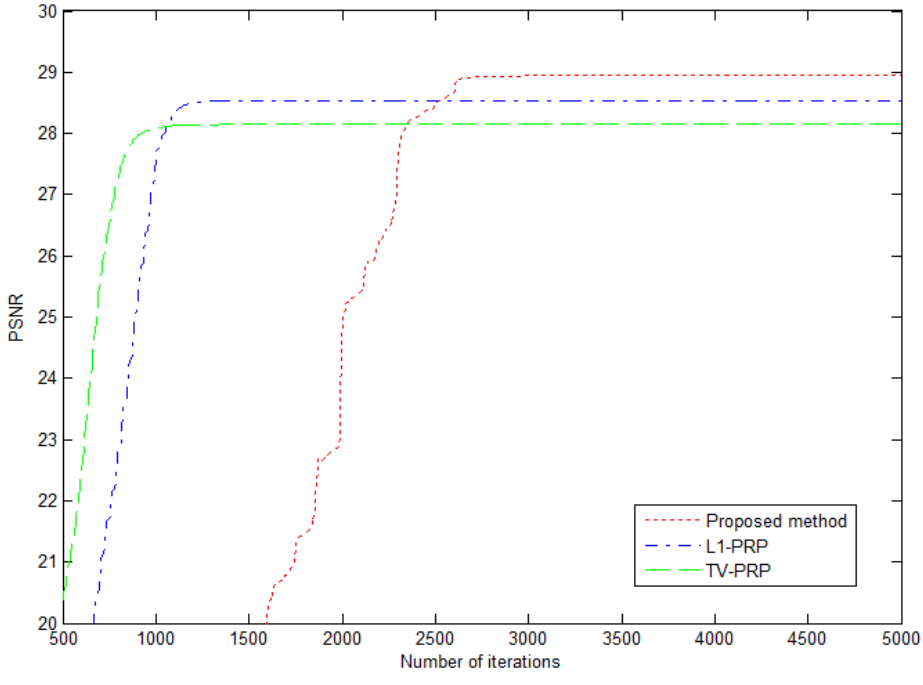

(a)

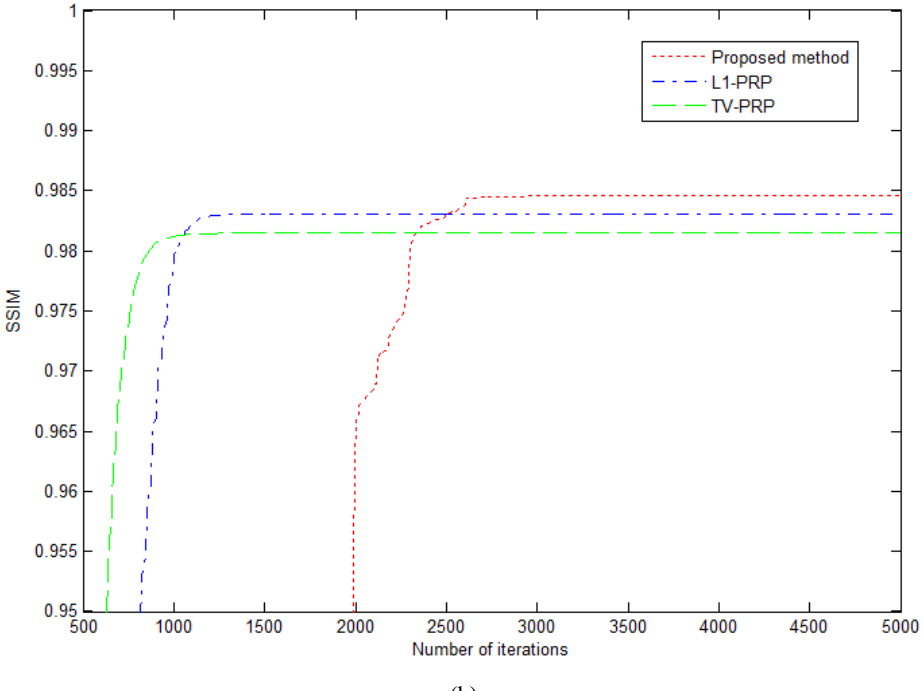

(b)

5 Conclusions

In this paper, the signal's sparsity and the target image's gradient variation are jointly considered. The least square method that combines L1 and TV regularisation is used to describe the image's objective function of compressive reconstruction. The approximate function is used as a substitute for the L1 norm and TV norm. The image is then reconstructed through a modified conjugate gradient algorithm. The proposed method is based on matrices and vectors only and is thus easy to implement. PSNR and SSIM are used as objective assessment indicators for reconstructed image. The experimental results show that after a certain number of iterations, the proposed method provides visually similar results but is more effective in terms of PSNR and SSIM than the L1_PRP algorithm that combines L1 norm and PRP and the TV_PRP algorithm that combines TV norm and PRP.

Future work will study compressive reconstruction experiments conducted on larger images. More efficient approximation functions and more efficient optimisation algorithms will be integrated to improve the algorithm's efficiency. Moreover, the method proposed in this paper for calculation of βk will be improved in order to reduce the number of iterations needed and to further improve the algorithm's efficiency.

Acknowledgements

The work in this paper is supported by the Guangxi Science and Technology Projects for Colleges and Universities (YB2014356), Guangxi Young and Middle-aged Teachers Basic Ability Promotion Projects for Colleges and Universities (2017KY0627) and Wuzhou University Key Projects (2012B004).

References

Beck, A. and Teboulle, M. (2009) 'Fast gradient-based algorithms for constrained total variation image denoising and deblurring problems', *IEEE Trans. Image Processing*, Vol. 18, No. 11, pp.2419–2434.

Candes, E.J., Romberg, J. and Tao, T. (2006) 'Robust uncertainty principle: exact signal reconstruction from highly incomplete frequency information', *IEEE Trans. on Information Theory*, Vol. 52, No. 2, pp.489–509.

Chen, F.H. and Li, S.A. (2016) 'The application of a modified HS conjugate gradient method for large-scale signal reconstruction problem', *Journal of Mathematics*, Vol. 36, No. 6, pp.1291–1298, in Chinese.

Chen, J., Shu, K.X., Yang, X.Z., Zheng, M.K. and Lin, L.Q. (2016a) 'Block-wise compression sensing reconstruction algorithm based on variational model', *Journal on Communications*, Vol. 37, No. 1, pp.101–109.

Chen, W.F., Li, S.D. and Yang, J. (2016b) '2D Complex sparse reconstruction algorithm with LBI and its application', *Acta Automatica Sinica*, Vol. 42, No. 4, pp.556–564.

Cheng, W.Y. and Liu, Q.F. (2010) 'Sufficient descent nonlinear conjugate gradient methods with conjugacy conditions', *Number Algor.*, Vol. 53, No. 1, pp.113–131.

Donoho D. (2006a) 'Compressed sensing', *IEEE Trans. on Information Theory*, Vol. 52, No. 4, pp.1289–1306.

Donoho, D.L. (2006b) 'For most large underdetermined systems of linear equations the minimal l1-norm solution is also the sparsest solution', *Communications on Pure and Applied Mathematics*, Vol. 59, No. 6, pp.797–829.

Donoho, D.L. and Tsaic, Y. (2006) 'Extensions of compressed sensing', *Signal Processing*, Vol. 86, No. 3, pp.533–548.

Figueiredo, M., Nowak, R.D. and Wright, S.J. (2007) 'Gradient pojection for sparse reconstruction: application to compressed sensing and other inverse problems', *Journal of Selected Topics in Signal Processing*, Vol. 1, No. 4, pp.586–598.

Ibrahim, S.M., Mustafa, M., Abdelrhaman, A., Mohd, R. and Zabidin, S. (2015) 'A modified nonlinear conjugate gradient method for unconstrained optimization', *Applied Mathematical Sciences*, Vol. 9, No. 54, pp.2671–2682.

Jeevan, K.P., Lu, W.S. and Antoniou, A. (2013) 'A new algorithm for compressive sensing based on total-variation norm', *IEEE Int. Symp. on Circuits and Systems (ISCAS)*, pp.1352–1355.

Zhang, J., Liu, S., Xiong, R. and Ma, S. (2012) 'Improved total variation based image compressive sensing recovery by nonlocal regularization', *Proceedings, IEEE International Symposium on Circuits and Systems (ISCAS)*, pp.2836–2839.